This article has been accepted for publication in a future issue of this journal, but has not been fully edited. Content may change prior to final publication. Citation information: DOI 10.1109/LMWC.2021.3062825, IEEE Microwave and Wireless Components Letters

A Monolithic Vertical Integration Concept for Compact Coaxial-Resonator-Based Bandpass Filters Using Additive Manufacturing

Kunchen Zhao, *student member, IEEE* and Dimitra Psychogiou *Member, IEEE*

***Abstract*—This paper reports on a compact, low-cost and low-loss monolithic integration concept for additively-manufactured coaxial-resonator-based bandpass filters (BPFs). Size compactness and low weight are achieved by vertically-stacking capacitively-loaded coaxial resonators and by monolithic integration that eliminates the need for assembly screws or fixtures. Furthermore, the proposed vertical integration concept allows for: i) flexible cross couplings to be realized enabling highly-selective transfer functions through transmission zero (TZ) generation and ii) for fairly complex geometries to be manufactured using low-cost stereolithography apparatus (SLA). For proof-of-concept demonstration purposes, a two-pole BPF with fractional bandwidth (FBW) of 8.5% and a three-pole/one-TZ BPF with FBW 6.2% at 3.8 GHz were designed, SLA-manufactured and measured. They exhibited low-levels of insertion loss (< 0.1 dB), high effective quality factors > 1,833 and wide spurious-free operation.**

***Index Terms*— Additive manufacturing, bandpass filters, coaxial cavity resonators, coaxial cavity filters, high-*Q* filters**

I. Introduction

Additive manufacturing (AM) techniques such as those based on fused deposition modelling (FDM), stereolithography apparatus (SLA), and selective laser sintering (SLS) have been increasingly explored as a low-cost and low-weight manufacturing alternative for RF components and subsystems of base stations and communication systems [1], [2]. Although at their infancy, AM technologies have already demonstrated their suitability for complex geometries [1] that are not manufacturable with conventional CNC machining or electron discharge machining (EDM). However, their manufacturing capabilities have not yet been exploited at their full potential. Most of the 3D coaxial or waveguide-based RF components and subsystems are manufactured as split-blocks of conventional textbook-based designs and assembled via screws or fixtures limiting their operation to low frequencies and increasing their size/weight.

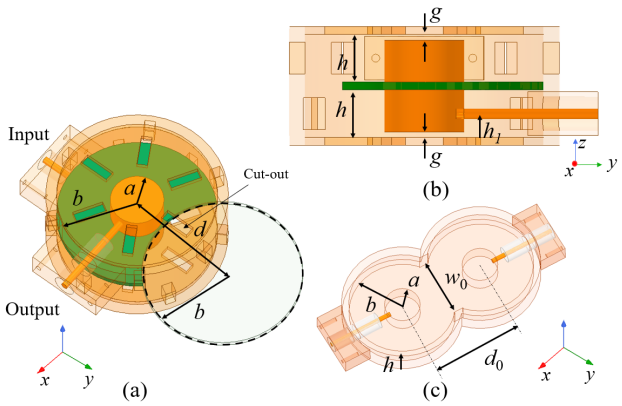

Fig 1. 3D EM model of the vertically-integrated coaxial resonator-based two-pole BPF. (a) Top view. (b) Side view and (c) 3D EM model of a conventional two-pole in-line coaxial BPF. The design parameters are: $a = 5$, $b = 15$, $d = 20.5$, $h = 6$, $g = 0.72$, $h_1 = 3$, $d_0 = 25$, $w_0 = 19.5$ all units are in mm.

Recent research efforts are focusing on the exploitation of AM for the miniaturization of the RF front-end. For example, in [3], new types of SLA-manufactured spherical-resonator-based bandpass (BPFs) are presented allowing for highly-versatile transfer functions. Complex coaxial-resonator filter topologies that are hard to realize with CNC machining are shown in [4] for the case of vertically-integrated conical resonator-based BPFs. Despite leading to reduced volume architectures, they exhibited high insertion loss (1.3 dB) and low effective quality factor (Q_{eff} ~100) due to the split-block integration approach that was prone to radiation losses. Monolithic integration of AM components and subsystems is also being explored to reduce the size and improve the RF performance of the front-end. However, most of these concepts are focused on waveguide-based configurations [5]-[9], which are relatively straightforward to metalize. Despite coaxial-based RF components (e.g., filters) being preferred for RF applications where broadband bandwidth, compact size and spurious free performance are critical, there exist a very limited number of coaxial AM components [10]-[15] and most of them are realized as split-blocks, as for examples the BPFs in [11]-[15].

Taking into consideration the aforementioned limitations, and the need for high quality factor (Q) and compact RF filters,

Manuscript received February 18th, 2021.

K. Zhao is with the Department of Electrical, Computer and Energy Engineering, University of Colorado, Boulder, CO 80309, USA (email: kunchen.zhao@colorado.edu).

D. Psychogiou is with the Department of Electrical, Computer, and Energy Engineering, University of Colorado Boulder, Boulder, CO 80309, USA, the Department of Electrical and Electronic Engineering, University College Cork, and Tyndall National Institute, Cork, Ireland (email: DPsychogiou@ucc.ie).

This article has been accepted for publication in a future issue of this journal, but has not been fully edited. Content may change prior to final publication. Citation information: DOI 10.1109/LMWC.2021.3062825, IEEE Microwave and Wireless Components Letters

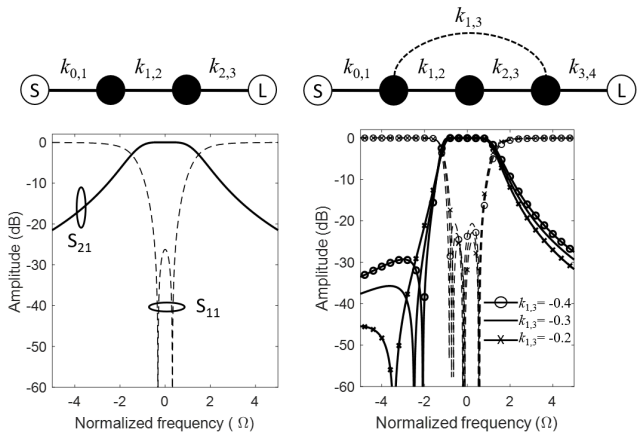

Fig 2. CRD and synthesized response. (a) Two-pole BPF ($k_{0,1} = k_{2,3} = 1$, $k_{1,2} = 0.8$). (b) Three-pole/one-TZ BPF ($k_{0,1} = k_{3,4} = 1$, $k_{1,2} = k_{2,3} = 0.7$). White circles: source and load; black circles: resonating nodes; solid lines: inter-resonator coupling; dashed line: cross coupling.

this paper explores for the first time a monolithic integration concept for coaxial-resonator-based BPFs that best occupy a 3D volume. In particular, the paper investigates a new class of vertically-stacked coaxial resonator-based arrangements that are seamlessly integrated and allow for low-loss and low-weight configurations. Furthermore, the proposed vertical integration concept allows for flexible cross couplings to be integrated, enabling the realization of highly-selective transfer functions through transmission zero (TZ) generation.

II. Filter Concept and Design Characteristics

The details of the vertically-stacked coaxial-resonator-based concept are illustrated in Fig. 1 through the example case of a two-resonator BPF that functionalizes the second-order coupling routing diagram (CRD) in Fig. 2(a). In particular, two capacitively-loaded coaxial resonators are stacked on top of each other which can be also viewed as folding a conventional two-pole in-line coaxial BPF around the iris of the inter-resonator coupling [see Fig. 1(c)]. Whereas the external coupling is materialized by tapping the inner conductor of the SMA in the post of the coaxial resonator, the inter-resonator coupling $k_{1,2}$ is provided by the circularly-shaped coupling window in the shared folded ground of the two resonators. The window is created by subtracting from the ground a circle with radius b and center distance of d to the resonator. Fig. 3(a) demonstrates the relationship between the $k_{1,2}$ and d which

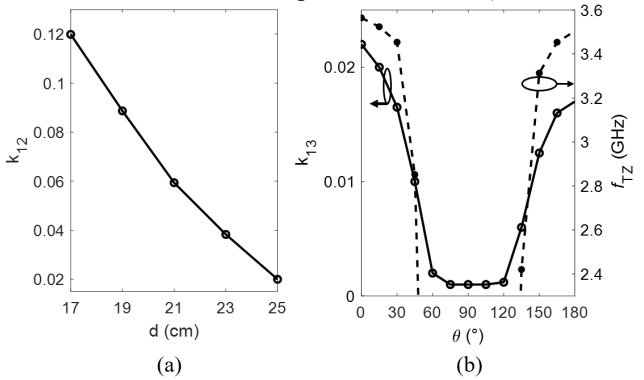

Fig 3. (a) $k_{1,2}$ as a function of d. and (b) $k_{1,3}$ and f_{TZ} as a function of θ.

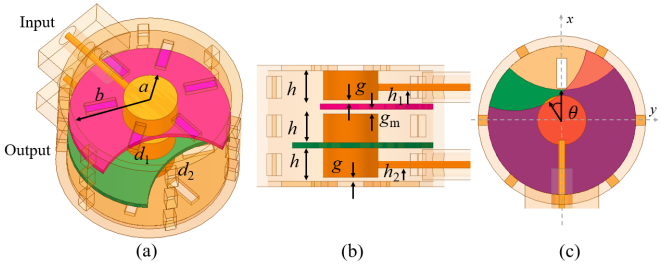

Fig 4. (a). 3D model of the proposed folded 3rd order coaxial cavity filter, (b) side view, and (c) top view. The critical design parameters are: $a = 5$, $b = 15$, $d_1 = 19.5$, $d_2 = 21.1$, $h = 6$, $g = 0.72$, $g_m = 0.82$, $h_1 = h_2 = 3$, all units are in mm. For the purpose of clear demonstration, $\theta = 30°$ in this plot, however in the designed prototype, the actual $\theta = 0°$ to maximize the $k_{1,3}$.

decreases with the increase of d and can be used as a reference for the design of the BPF transfer function.

To illustrate the merits of vertical stacking in terms of uniform utilization of a 3D volume, a conventional two-pole in-line coaxial BPF and the proposed vertically-stacked coaxial-resonator-based BPF were designed for a center frequency of 3.8 GHz and fractional bandwidth (FBW) or 8.5% (their dimensions are listed in Fig. 1) and compared against their aspect ratios (AR)—AR is defined as the ratio of the largest dimension of a component in the x-y plane over its height. Based on this metric, a BPF with a cubical shape would be the most preferred configuration with a minimum AR of $2^{0.5}$. Using as a basis the dimensions listed in Fig. 1, the in-line coaxial BPF has an AR of 9.07 whereas the proposed vertically-stacked coaxial BPF has an AR of 2.27 which is about 4x smaller.

A. Scalability to advanced transfer functions

To demonstrate the scalability of the vertical coaxial-resonator-based integration concept to advanced transfer functions and geometrical configurations, a three-pole/one-TZ architecture was explored using as a basis the CRD model and its corresponding synthesized response in Fig. 2(b). The 3D EM model of the filter and resulting vertically-integrated configuration is shown in Fig. 4. The circular-shaped coupling element was also used in this case, where the center distance of the coupling window is denoted by d_1 and d_2 (Fig. 4a) in the same manner as in the two-pole case. Furthermore, we investigated the potential to introduce cross coupling between the first and the third resonator $k_{1,3}$ with the purpose of generating a TZ. This is achieved by rotating the relative angle θ between the two coupling windows, as shown in Fig. 4(c), which in turn controls the coupling strength and the spectral

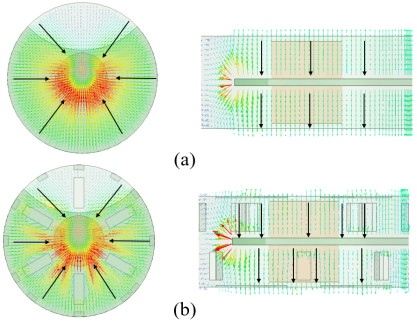

Fig 5. Surface current distribution for the vertically-integrated two-pole BPF at 3.5 GHz. (a) Without slots and (b). with slots. Left: top view, right: side view, black lines indicate the direction of current.

This article has been accepted for publication in a future issue of this journal, but has not been fully edited. Content may change prior to final publication. Citation information: DOI 10.1109/LMWC.2021.3062825, IEEE Microwave and Wireless Components Letters

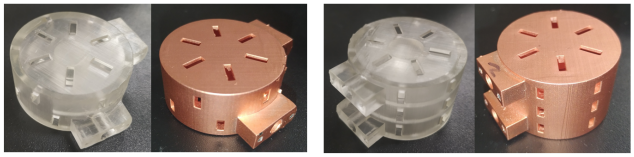

(a) (b)

Fig 6. Manufactured prototypes. (a) Two-pole BPF. (b) Three-pole/one-TZ BPF. Left: before Cu-plating; right: after Cu-plating.

location of the TZ f_{TZ} as shown in Fig. 3(b). Using as a basis the 3D BPF geometry in Fig. 4 and the inter-resonator coupling parametric studies in Fig. 3, a three-pole/one-TZ BPF was designed for a center frequency of 3.8 GHz, FBW of 6.2% and a TZ located at 3.56 GHz. The geometrical dimensions of the filter are listed in Fig. 4 and correspond to an AR of 1.54 that is 8x smaller than the AR of 12.2 that of a conventional three-pole in-line conventional coaxial BPF would exhibit. Moreover, the in-line configuration does not allow for TZ generation due to the difficulty to create the $k_{1,3}$ cross coupling.

B. Practical realization aspects

To facilitate monolithic integration of the vertically-integrated coaxial-resonator-based BPFs, SLA manufacturing is considered due to allowing for smooth surfaces and high-resolution. To facilitate Cu-platting without having to dissect the filter into multiple parts, slots need to be added on the surfaces of the BPFs to allow for the Cu-platting solution to flow within the filter volume. It is important to select the slot dimensions, sizes and orientations so that they do not radiate at the operational frequency range of the filter. To minimize their impact, the surface current of the filter is analyzed using the eigen-mode solver of HFSS. As shown in Fig. 5(a), the current on the top of the cavity is distributed along the radial direction, while the current on the side wall is distributed along the vertical direction. Thus, rectangular-type slots that are in parallel to the current direction are the most appropriate ones. This is verified in Fig. 5(b) which shows that the current pattern remains unchanged after adding the slots along the current lines.

III. Experimental Validation

To validate the practical viability of the vertically-stacked monolithic integration concept, a two-pole and a three-pole/one TZ BPF prototypes were designed for a center frequency of 3.8 GHz and FBWs of 8.5 and 6.2 % respectively. The filters were manufactured with a desktop SLA 3D printer (50 μm layer

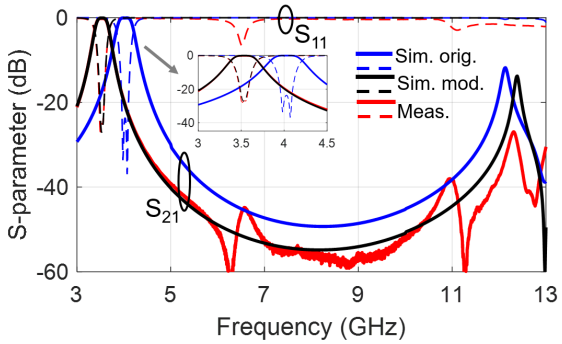

Fig 7. RF-measured and EM-simulated S-parameters of the two-pole vertically-stacked coaxial-resonator-based BPF.

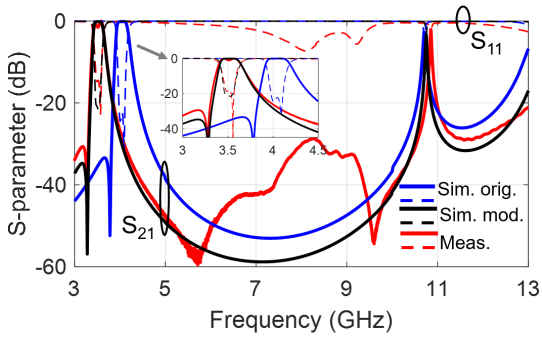

Fig 8. RF-measured and EM-simulated S-parameters of the three-pole/one-TZ vertically-stacked coaxial-resonator-based BPF.

thickness) and were Cu-plated with a commercially-available electroless process. A Cu-platting thickness of 50 μm was selected to reduce conductive losses. The fabricated prototypes before and after Cu-plating are shown in Fig. 6.

The RF measured S-parameters of the two-pole and the three-pole/one-TZ BPFs are shown in Fig. 7 and 8. Their corresponding EM simulated responses are also provided in these figures. The observed frequency shift is attributed to the manufacturing tolerance, especially in the capacitive gap (g in Fig. 1(b)). This is verified by reducing g by 0.1 mm in the simulation (shown in Fig. 7, 8), which shows an excellent agreement with the measurement. Although the same tolerance may apply to x-y dimensions, it does not have a significant impact on the overall response. The RF measured performance parameters of the BPFs are summarized as follows. Two-pole BPF: center frequency of 3.53 GHz, minimum in-band IL of 0.08 dB (corresponds to a Q_{eff} of 1833), FBW of 8.8%, spurious-free operation up to 12.4 GHz and only 11 gr of weight. Three-pole/one-TZ BPF: center frequency 3.51 GHz, minimum in-band IL of 0.09 dB (Q_{eff} of 2461), FBW of 6.7%, a TZ at 3.27 GHz, spurious-free performance up to 11 GHz and 15 gr of weight. The aforementioned RF performance is comparable to the one of fully-metal in-line coaxial CNC machined filters. However, the proposed approach allows for significantly smaller AR, lighter weight and lower cost. If compared to AM coaxial filters, the proposed approach demonstrates significantly higher Q_{eff} (Q_{eff} in [4] is about 100 and in [8] is between 500-950). Furthermore, in relation to the split-block approach in [4], it has comparable AR, however the proposed filter concept exhibits significantly higher Q_{eff} and operational frequency due to its monolithic integration. Furthermore, it has been applied to higher-order transfer functions and has demonstrated the potential to incorporate TZs.

IV. Conclusion

A new type of additively-manufactured coaxial-resonator-based BPFs is reported. The proposed monolithic vertical integration concept allows for low-loss (Q_{eff}> 1833) and low-weight (11-15 gr) vertically-stacked coaxial-filters that effectively occupy a given 3D space. Furthermore, it allows for flexible cross couplings to be readily embedded and exploited for the realization of TZs. The concept was validated at S-band through the manufacturing and testing of an SLA-manufactured two-pole and a three-pole/one TZ BPFs.

REFERENCES

[1] W. J. Otter and S. Lucyszyn, "3-D printing of microwave components for 21st century applications," *2016 IEEE MTT-S International Microwave Workshop Series on Advanced Materials and Processes for RF and THz Applications (IMWS-AMP)*, Chengdu, 2016, pp. 1-3.

[2] B. Zhang, R. Li, L. Wu, H. Sun and Y. Guo, "A highly integrated 3-D printed metallic K-band passive front end as the unit cell in a large array for satellite communication," in *IEEE Antennas and Wireless Propagation Letters*, vol. 17, no. 11, pp. 2046-2050, Nov. 2018.

[3] C. Guo, X. Shang, M. J. Lancaster and J. Xu, "A 3-D printed lightweight X-band waveguide filter based on spherical resonators," in *IEEE Microwave and Wireless Components Letters*, vol. 25, no. 7, pp. 442-444, July 2015.

[4] E. López-Oliver et al., "3-D printed bandpass filter using conical posts interlaced vertically," *2020 IEEE/MTT-S International Microwave Symposium (IMS)*, Los Angeles, CA, USA, 2020, pp. 580-582.

[5] Y. Zhang, F. Zhang, Y. Gao, J. Xu, C. Guo and X. Shang, "3D printed waveguide step-twist with bandpass filtering functionality," in *Electronics Letters*, vol. 56, no. 11, pp. 527-528, 28 5 2020.

[6] B. T. W. Gillatt, M. D'Auria, W. J. Otter, N. M. Ridler and S. Lucyszyn, "3-D printed variable phase shifter," in *IEEE Microwave and Wireless Components Letters*, vol. 26, no. 10, pp. 822-824, Oct. 2016.

[7] C. Guo, J. Li, J. Xu and H. Li, "An X-band lightweight 3-D printed slotted circular waveguide dual-mode bandpass filter," *2017 IEEE International Symposium on Antennas and Propagation & USNC/URSI National Radio Science Meeting*, San Diego, CA, 2017, pp. 2645-2646.

[8] F. L. Borgne, G. Cochet, J. Haumant, D. Diedhiou, K. Donnart and A. Manchec, "An integrated monobloc 3D printed front-end in Ku-band," *2019 49th European Microwave Conference (EuMC)*, Paris, France, 2019, pp. 786-789, doi: 10.23919/EuMC.2019.8910891.

[9] J. Li, C. Guo, L. Mao, J. Xiang, G. Huang and T. Yuan, "Monolithically 3-D printed hemispherical resonator waveguide filters with improved out-of-band rejections," in *IEEE Access*, vol. 6, pp. 57030-57048, 2018.

[10] K. Zhao and D. Psychogiou, "Monolithic SLA-based capacitively-loaded high-Q coaxial resonators and bandpass filters," *2020 50th European Microwave Conference (EuMC)*, Utrecht, Netherlands, 2021, pp. 471-474.

[11] C. Tomassoni, G. Venanzoni, M. Dionigi and R. Sorrentino, "Compact quasi-elliptic filters with mushroom-shaped resonators manufactured with 3-D Printer," in *IEEE Trans. on Microw. Theory Techn.*, vol. 66, no. 8, pp. 3579-3588, Aug. 2018.

[12] K. Sadasivan and D. Psychogiou, "Tunable 3D-printed coaxial-cavity filters with mixed electromagnetic coupling," *2019 IEEE International Symposium on Antennas and Propagation and USNC-URSI Radio Science Meeting*, Atlanta, GA, USA, 2019, pp. 1703-1704.

[13] G. Venanzoni, C. Tomassoni, M. Dionigi and R. Sorrentino, "Stereolitographic 3D printing of compact quasi-elliptical filters," *2017 IEEE MTT-S International Microwave Workshop Series on Advanced Materials and Processes for RF and THz Applications (IMWS-AMP)*, Pavia, 2017, pp. 1-3.

[14] G. Venanzoni, M. Dionigi, C. Tomassoni and R. Sorrentino, "3-D-printed quasi-elliptical evanescent mode filter using mixed electromagnetic coupling," in *IEEE Microwave and Wireless Components Letters*, vol. 28, no. 6, pp. 497-499, June 2018.

[15] C. Tomassoni, G. Venanzoni, M. Dionigi and R. Sorrentino, "Compact doublet structure for quasi-elliptical filters using stereolitographic 3D printing," *2017 47th European Microwave Conference (EuMC)*, Nuremberg, 2017, pp. 993-996.